1-1-2012

Spectral engineering of optical fiber preforms through active nanoparticle doping

T. Lindstrom

E. Garber

D. Edmonson

T. Hawkins

Y. Chen
University of Central Florida

See next page for additional authors

Spectral engineering of optical fiber preforms through active nanoparticle doping

T. Lindstrom,[1] E. Garber,[1] D. Edmonson,[1] T. Hawkins,[1] Y. Chen,[2] G. Turri,[2] M. Bass,[2] and J. Ballato[1,*]

[1]*Center for Optical Materials Science and Engineering Technologies (COMSET) and the Department of Materials Science and Engineering, Clemson University, Clemson, SC 29631, USA*
[2]*CREOL, The College of Optics and Photonics, University of Central Florida, Orlando, FL 32816, USA*
**jballat@clemson.edu*

Abstract: Europium doped alkaline earth fluoride [Eu:AEF_2 (AE = Ca, Sr, Ba)] nanoparticles were synthesized and systematically incorporated into the core of modified chemical vapor deposition (MCVD)-derived silica-based preforms by solution doping. The resulting preforms were examined to determine the impact of the nanoparticles chemistry on the spectroscopic behavior of the glass. The dominant existence of Eu^{3+} was demonstrated in all preforms, which is in contrast to conventional solution doped preforms employing dissolved europium salts where Eu^{2+} is primarily observed. Raman spectroscopy and fluorescence lifetime measurements indicated that the nanoparticles composition is effective in controlling, at a local chemical and structural level, the spectroscopic properties of active dopants in optical fiber glasses. Further, there is a systematic and marked increase in radiative lifetime, τ, of the Eu^{3+} emission that follows the cationic mass; $\tau_{Ca} < \tau_{Sr} < \tau_{Ba}$ with the BaF_2-derived sample yielding a 37% lengthening of the lifetime over the CaF_2-derived one. Such nanoscale control of what otherwise is silica glass could be useful for realizing property-enhanced and tailored spectroscopic performance from otherwise "standard" materials, e.g., vapor-derived silica, in next generation optical fibers.

OCIS codes: (160.2290) Fiber materials; (060.2290) Fiber materials; (060.2310) Fiber optics.

References and links

1. D. Richardson, J. Nilsson, and A. Clarkson, "High power fiber lasers: current status and future perspectives [Invited]," J. Opt. Soc. Am. B **27**(11), B63–B92 (2010).
2. A. Bjarklev, *Optical Fiber Amplifiers: Design and System Applications* (Artech House, 1993).
3. S. Poole, D. Payne, and M. Fermann, "Fabrication of low-loss optical fibres containing rare earth ions," Electron. Lett. **21**(17), 737–738 (1985).
4. J. Townsend, S. Poole, and D. Payne, "Solution-doping technique for fabrication of rare earth doped optical fibres," Electron. Lett. **23**(7), 329–331 (1987).
5. V. Khopin, A. Umnikov, A. Gur'yanov, M. Bubnov, A. Senatorov, and E. Dianov, "Doping of optical fiber preforms via porous silica layer infiltration with salt solutions," Inorg. Mater. **41**(3), 303–307 (2005).
6. A. Dhar, A. Pal, M. Ch. Paul, P. Ray, H. S. Maiti, and R. Sen, "The mechanism of rare earth incorporation in solution doping process," Opt. Express **16**(17), 12835–12846 (2008).
7. M. Digonnet, ed., *Rare-Earth-Doped Fiber Lasers and Amplifiers* (Marcel Dekker, Inc., 2001).
8. S. Tammela, M. Soderlund, J. Koponen, V. Philippov, and P. Stenius, "The potential of direct nanoparticle deposition for the next generation of optical fibers," Proc. SPIE **6116**, 61160G (2006).
9. W. Blanc, B. Dussardier, G. Monnom, R. Peretti, A. M. Jurdyc, B. Jacquier, M. Foret, and A. Roberts, "Erbium emission properties in nanostructured fibers," Appl. Opt. **48**(31), G119–G124 (2009).
10. W. Blanc, D. Dussardier, and M. Paul, "Er-doped oxide nanoparticles in silica-based optical fibers," Phys. Chem. Glasses **A50**, 79–81 (2009).
11. B. Dussardier, W. Blanc, and G. Monnom, "Luminescent ions in silica-based optical fibers," Fiber Integr. Opt. **27**(6), 484–504 (2008).
12. A. Céreyon, A. Jurdyc, V. Martinez, E. Burov, A. Pastouret, and B. Champagnon, "Raman amplification in nanoparticles doped glasses," J. Non-Cryst. Solids **354**(29), 3458–3461 (2008).
13. O. Podrazky, I. Kasik, M. Pospisilova, and V. Matejec, "Use of nanoparticles for preparation of rare-earth doped silica fibers," Phys. Status Solidi C **6**(10), 2228–2230 (2009).

#174771 - $15.00 USD Received 23 Aug 2012; revised 24 Sep 2012; accepted 26 Sep 2012; published 1 Oct 2012

14. D. Boivin, T. Föhn, E. Burov, A. Pastouret, C. Gonnet, O. Cavani, C. Collet, and S. Lempereur, "Quenching investigation on new erbium doped fibers using MCVD nanoparticle doping process," Proc. SPIE **7580**, 75802B (2010).
15. C. Kucera, B. Kokuoz, D. Edmondson, D. Griese, M. Miller, A. James, W. Baker, and J. Ballato, "Designer emission spectra through tailored energy transfer in nanoparticle-doped silica preforms," Opt. Lett. **34**(15), 2339–2341 (2009).
16. K. Oh, T. Morse, L. Reinhart, A. Kilian, and W. Risen, Jr., "Spectroscopic analysis of a Eu-doped aluminosilicate optical fiber preform," J. Non-Cryst. Solids **149**(3), 229–242 (1992).
17. C. Pandey, S. Dhopte, P. Muthal, V. Kondawar, and S. Moharil, "$Eu^{3+} \leftrightarrow Eu^{2+}$ redox reactions in bulk and nano CaF_2:Eu," Radiat. Eff. Defects Solids **162**(9), 651–658 (2007).
18. J. DiMaio, B. Kokuoz, T. L. James, T. Harkey, D. Monofsky, and J. Ballato, "Photoluminescent characterization of atomic diffusion in core-shell nanoparticles," Opt. Express **16**(16), 11769–11775 (2008).
19. Y. Nageno, H. Takebe, K. Morinaga, and T. Izumitani, "Effect of modifier ions on fluorescence and absorption of Eu^{3+} in alkali and alkaline earth silicate glasses," J. Non-Cryst. Solids **169**(3), 288–294 (1994).
20. J. Frantza and B. Mysen, "Raman spectra and structure of $BaO-SiO_2$, $SrO-SiO_2$, and $CaO-SiO_2$ melts to 1600C," Chem. Geol. **121**(1-4), 155–176 (1995).

1. Introduction

With growing demand for active optical fibers [1], numerous methods have been developed to incorporate rare earth ions into the core of the precursor glass preform [2–5]. Two primary processes have been favored: vapor phase doping [3] and solution doping [4] as an additional step to the chemical vapor deposition, e.g., MCVD, OVD, silica preform process.

In the case of solution doping [4], which is most common commercially, the core soot layers are deposited at a reduced temperature in order to produce a partially-sintered porous body. The soot-filled tube then is removed from the lathe and aqueous solutions of the desired dopant precursors are drawn into the center of the tube, allowed to soak, drained and dried. The doped soot tube then is returned to the lathe and the soot is subsequently sintered and collapsed into the final doped preform.

Much work has been conducted to optimize the uniformity of doping, the effect of solvents used, and the desired doping concentrations [5,6]. Low rare earth solubility in silica glass, which facilitates clustering and enhanced ion-ion interactions, results in both a difficulty to incorporate large quantities of lanthanide ions into the rigid SiO_2 network as well as reduced spectroscopic performance from those dopants that are incorporated. The use of glass network intermediates or modifiers, such as alumina (Al_2O_3) and phosphate (P_2O_5), has been critical to the realization of preforms, hence optical fibers, exhibiting better control of rare earth concentration and profile within the core with less detrimental ion-ion interactions [7]. These modified glasses allow for higher concentrations of rare earth dopants without clustering effects as the modifier ions 'open up' the silicate structure which aids in lanthanide solubility.

More recently, several studies have considered the use of nanoparticles, rather than dissolved salts, as a route to solution doped glasses. For example, Liekki Corporation has developed the "Direct Nanoparticle Deposition" (DND) technology [8], in which outside chemical vapor deposition (OVD) generally is employed but glass particles are formed using atomized liquid raw materials. The particles comprised, formed through evaporation/condensation processes, are between about 10-100 nm in size, can be evenly distributed along the length of the preform, and are reported to result in enhanced absorption and emission cross-sections due to the more highly doped core compositions.

Blanc, et al. [9,10], and Dussadier [11], have developed a method where commercially-available nanopowders of rare earth chlorides and calcium chloride are used in the soaking solution to incorporate Ca^{2+} and Er^{3+} ions into an MCVD-derived preform by solution doping. During the subsequent high temperature processing, germania and phosphorous are added to the core and doped particles are formed *in situ* in the size range of 100-250 nm. This technique is an extension of particles grown in bulk silicate glasses containing Cd-S-Se, where Cd nanoparticles of 2-6 nm are grown in commercially made borosilicate glasses during annealing at 650°C [12]. The fibers prepared to-date have high losses due to scattering and the average nanoparticle size is considered too large to allow for acceptable transmission.

#174771 - $15.00 USD Received 23 Aug 2012; revised 24 Sep 2012; accepted 26 Sep 2012; published 1 Oct 2012

Podrasky, et al. [13], and Boivin, et al. [14], report similar methods to Blanc, using doped alumina nanopowders during the solution doping step. These nanoparticles are produced during the high temperature sintering process of MCVD and are reported to improve the intensity of erbium emissions in comparison to conventionally-solution doped preforms due to reduced quenching by virtue of better homogeneity within the preform.

Kucera, et al. [15], studied the solution doping of Tb^{3+}- and Eu^{3+}-doped lanthanum fluoride, LaF_3, nanoparticles to determine if differently-doped nanoparticles could be incorporated into the same glass but not interact with one another because each dopants should largely remain localized to the region where its nanoparticle resides. The resulting glass produced tailored emission spectra that validated the generalized concept of spectral engineering through nanoparticle doping.

This work is an extension of Kucera, et al. [15], and seeks to expand the understanding of the role of nanoparticle doping on the spectroscopy of the resultant all-glass preforms. In common with [15] is the use of the europium ion as a spectroscopic probe into local glass structure given its well-studied hypersensitive electrical dipole and magnetic dipole visible emissions as well as the phonon sideband associated with its zero phonon line excitation; also in the visible. Different from [15] is the use of alkaline earth fluoride nanoparticles, AEF_2 (AE = Ca, Sr, Ba), to permit a systematic study of the influence of nanoparticle chemistry, i.e., cation in this case, on the resultant spectroscopic properties of the silica preform. If the local surroundings/environment about the rare earth ion can influence the emission characteristics in an otherwise "conventional" silica preform, then one has enabled considerably greater flexibility in the spectroscopic properties of silica-based active optical fiber without significantly modifying the processing methods and conditions.

2. Experimental procedures

2.1 Nanoparticle synthesis and characterization

Alkaline earth nitrate, $AE(NO_3)_2$, (Alfa Aesar), where AE = Ca, Sr, or Ba, was dissolved in deionized water and added drop-wise at a rate of ~0.5 ml/min, to a solution of 175 ml of 1:1 water:ethanol, 0.630g ammonium fluoride, (NH_4F), and 3.07g of ammonium di-n-octadecyldithiophosphate, (ADDP, $[NH_4]$-$[S_2P(OC_{18}H_{37})_2]$), maintained at 75°C. Following the complete addition of the nitration solution, the resulting mixture had a slightly turbid color and was allowed to stir at 250 rpm for 2 hours in a water bath at 75 °C. The solution was removed from the water bath and allowed to cool to room temperature. Europium doping was performed by adding $Eu(NO_3)_3$ into the aforementioned solution at a ratio of 5% by weight relative to the alkaline-earth cation; i.e., all nanoparticles were doped with 5 weight percent europium. The choice of the 5% europium-doping level is simply to provide a high enough quantity of Eu to observe the visible emissions with relative ease but not so high as to influence the structure of the alkaline earth nanoparticles.

2.2 X-ray diffraction (XRD)

In order to determine the crystallinity and verify the phase purity of the nanoparticles, x-ray diffraction was performed on the dried powders using a Scintag XDS 4000 and CuK_α radiation.

2.3 Transmission electron microscopy (TEM)

High resolution transmission electron microscopy (HRTEM) was performed on the nanoparticle powders to provide visual inspection of the particle size and morphology. Less than 0.001 g of each powder was suspended in ~10 ml of tetrahydrafuran (Acros, anhydrous, Acroseal, 99.9%), and a single drop of the solution was placed on a 200 mesh copper grid (Ted Pella, Inc.), allowed to dry and used for analysis. HRTEM was performed on a Hitachi H9500 operating at an accelerating voltage of 300kV.

#174771 - $15.00 USD Received 23 Aug 2012; revised 24 Sep 2012; accepted 26 Sep 2012; published 1 Oct 2012

2.4 Raman spectroscopy

The vibrational spectra of the alkaline earth fluorides nanoparticles was measured using a Senterra 178 Raman Microscope (Bruker Optics) operating at a laser wavelength of 532 nm, laser power of 20 mW and integration time of 100s.

2.5 Photoluminescence and radiative lifetime measurements

Emission and excitation spectra were collected on all the Eu:AEF_2 nanoparticle using a Jobin Yvon Fluorolog 3 specrofluorometer with a double grating configuration, an excitation bandpass of 2 nm and a scan rate of 0.1-1 nm/min. Emission scans were performed at an excitation wavelength of 393nm. Radiative lifetimes were measured using a 10 pulse per second, Q-switched, frequency tripled Nd:YAG laser pumped Spectra Physics MOPO Model 730 parametric oscillator to generate ~4 nsec pulses at the excitation wavelength of 464 nm. Emission excited by this light at 613 nm was selected with an Acton Model 300i spectrometer and detected with a fast photomultiplier. The signal was recorded with a digital oscilloscope and downloaded to a computer for analysis.

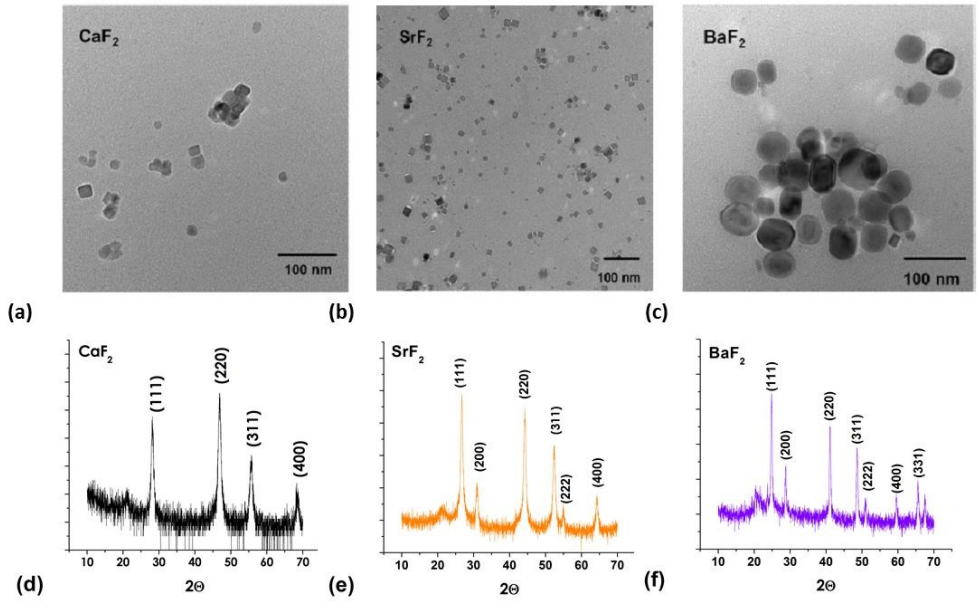

Fig. 1. Transmission electron micrographs of the as-synthesized (a) CaF_2, (b) SrF_2, and (c) BaF_2. Powder x-ray diffraction scans of the as-synthesized (d) CaF_2, (e) SrF_2, and (f) BaF_2 with crystallographic reflections noted.

2.6 MCVD fabrication of nanoparticle doped preforms

Four individually solution-doped preforms were fabricated containing either Eu:CaF_2, Eu:SrF_2, or Eu:BaF_2 nanoparticles as well as one prepared from a solution of dissolved europium and aluminum chloride salts. This latter preform was fabricated as a reference to compare the use of nanoparticles to conventional dissolved-salt solution doping. Modified chemical vapor deposition (MCVD) fabrication of the doped preforms was carried out using an SG Controls lathe (Clemson University) and processing conditions equivalent to those in [15]. The nanoparticles were individually suspended in anhydrous tetrahydrafuran (THF) to achieve a doping level of nanoparticles in solution of 0.1 M. The nanoparticles were batched by weight and added to 150 ml of THF, sonicated for 30 minutes to insure a uniform suspension and made approximately one hour before the solution doping step. This solution results in a preform which is doped to ~2500 parts per million of 5Eu:AEF_2 nanoparticles

#174771 - $15.00 USD Received 23 Aug 2012; revised 24 Sep 2012; accepted 26 Sep 2012; published 1 Oct 2012

(estimated values based on [4,5]). The conventional Eu_2O_3/Al_2O_3 dissolved salt solution was made to a ratio of 0.1 M/1 M in a solution containing equal parts water and ethanol.

3. Results and discussion

Figure 1 provides transmission electron micrographs and powder x-ray diffraction scans of the as-synthesized alkaline-earth fluoride nanoparticles confirming their nanoscale dimensions and phase purity, respectively. Further, as expected, the generally cubic shape of the alkaline-earth fluoride nanoparticles is observed. Image analysis of the TEM micrographs yielded average particles of 9.2 nm, 19.5 nm, and 24.3 nm for the CaF_2, SrF_2, and BaF_2 nanoparticles, respectively.

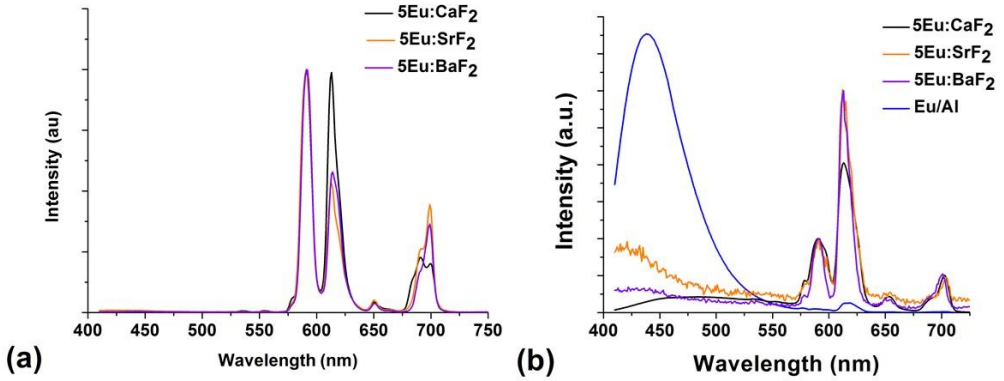

Fig. 2. (a) Emission spectra of precursor europium doped $(AE)F_2$ nanoparticles; *N.B.*, only present are emissions indicative of Eu^{3+}. (b) Emission spectra of the Eu:$(AE)F_2$ nanoparticle doped silica preforms; *N.B.*, only present are emissions indicative of Eu^{3+} in the nanoparticle-doped preforms whereas Eu^{2+} is found in the conventionally (dissolved salt) solution doped preform (Eu/Al). In all cases, the nanoparticles were doped with 5 weight percent Eu and the excitation wavelength was 393 nm.

The emission spectra (λ_{ex} = 393 nm) from the Eu:$(AE)F_2$ nanoparticles and the corresponding nanoparticle doped preforms are shown in Fig. 2. All spectra were normalized to the intensity of the $^5D_0 \rightarrow {}^7F_1$ magnetic dipole transition since such transitions are insensitive to the local chemical environment. The Eu in the as-made nanoparticles (Fig. 2(a)) emits characteristically at 590 nm ($^5D_0 \rightarrow {}^7F_1$) and 610 nm ($^5D_0 \rightarrow {}^7F_2$) as well as at about 650 nm ($^5D_0 \rightarrow {}^7F_3$) and 695 nm ($^5D_0 \rightarrow {}^7F_4$). While there are subtle differences between the relative emission intensities of the europium in each type of alkaline earth fluoride, the generalized emissions are clearly and unequivocally indicative of the trivalent state; i.e., Eu^{3+}.

In the Eu:$(AE)F_2$ nanoparticle-doped preforms, the emissions (Fig. 2(b)) are predominately those from the $^5D_0$ manifold of Eu^{3+}, with individual peaks at 590 nm ($^5D_0 \rightarrow {}^7F_1$), 610 nm ($^5D_0 \rightarrow {}^7F_2$), 650 nm ($^5D_0 \rightarrow {}^7F_3$) and ~700nm ($^5D_0 \rightarrow {}^7F_4$), which directly correlates to the emissions of the as-made nanoparticles. In contrast, the preform made using conventional dissolved Eu-salts exhibited emissions that correspond to the $4f^6 5d^1 \rightarrow 4f^7$ ($^8S_{7/2}$) transition of Eu^{2+} [16]. This stark change in emission behavior (Eu^{3+} vs. Eu^{2+}) indicates a distinct change in local environment for the Eu ion strongly suggesting that chemical aspects of the nanoparticle are present despite the processing of the preform at temperatures in excess of 2200°C. The Eu^{3+} emissions demonstrated by the preforms are reasonably similar to that of the heat treated, nanoparticle emissions, further substantiating the rare earth ion is 'insulated' from the surrounding silica matrix by the immediate surrounding remaining from their original nanoparticle host. For completeness, it is worth noting that thermal treatment of alkaline earth nanoparticles, though not contained within a glass, have been reported [17] and were shown to undergo conversion from the trivalent to divalent state when annealed above about 300 °C. The lack of such a valence conversion in this work suggests that the necessary

#174771 - $15.00 USD Received 23 Aug 2012; revised 24 Sep 2012; accepted 26 Sep 2012; published 1 Oct 2012

charge-compensation mechanisms remain present during the processing of the preform. Additionally, as noted, the preforms were processed in excess of 2200°C and exhibited only the Eu^{3+} spectral signatures. It is therefore unlikely that subsequent fiber drawing at a typical temperature of about 1950°C would further influence the europium valence state.

As an aside, with respect to potential scattering of propagating light through this nanoparticle "doped" glass, the largest nanoparticles (i.e., 24.3 nm) are only about 4% of the wavelength of the red Eu emission being used here as a spectroscopic probe. Some diffusion is known to occur [18] during the processing of the preform which inevitably grades the compositional, hence optical, differences between nanoparticle and glass "host." For these reasons, albeit qualitative, it is reasonable to expect that scattering is not especially problematic. Indeed, as shown in Fig. 2(b), there is some tailing off of the excitation signal observed at short wavelengths but this is measurably weaker than the Eu emission. Further, at wavelengths of practical interest, which are longer than those used here (e.g., 1 μm with Yb doping, 1.55 μm with Er doping) any scattering due to the presence of the nanoparticles would be further diminished.

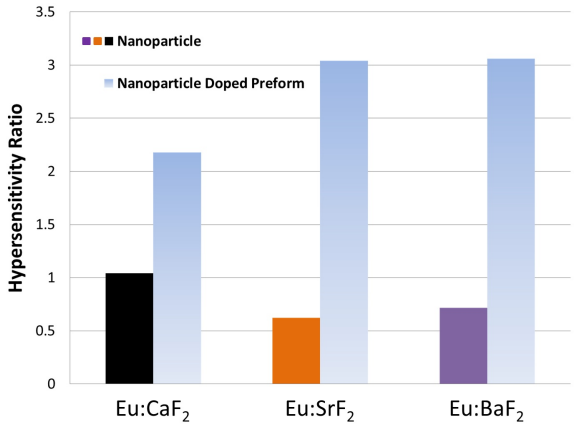

Fig. 3. Comparison of hypersensitivity ratio of europium (Eu^{3+}) doped alkaline earth fluoride nanoparticle to that from the same nanoparticle doped preform.

The hypersensitivity ratio, which is the integrated area under the hypersensitive electric dipole emission ($^5D_0 \rightarrow {}^7F_2$) to the magnetic dipole emission ($^5D_0 \rightarrow {}^7F_1$) and therefore is a good measure of the nature and symmetry of the rare earth ion within a host material, is provided in Fig. 3. Based on an examination of the hypersensitivity ratios associated with the nanoparticles relative to those from the corresponding preforms (Fig. 2), a distinct difference in the structural and chemical environment about the europium ion clearly is demonstrated. More specifically, since the hypersensitivity ratio is greater when site symmetries about the Eu^{3+} are more asymmetric, the change in hypersensitivity ratio between the doped nanoparticle and the corresponding nanoparticle doped preform suggests a structural environment that goes from more symmetric in the nanoparticle crystal to more asymmetric in the glass. In comparing the Eu:AEF_2 doped preforms, the change in local chemical environment for the europium ion becomes more evident as the SrF_2 and BaF_2 doped preforms appear to have similar hypersensitivity ratios, while the CaF_2 doped preform has a lower hypersensitivity ratio, indicating a slightly more ordered environment when compared to the other preforms. It is interesting to note that the change in hypersensitivity ratio is different in the case of the nanoparticles with respect to the preforms. Relative to the choice of cation (Ca $\rightarrow$ Sr $\rightarrow$ Ba), the ratio is found to decrease in the nanoparticles but increase in the preforms. Though not the same glass system, the hypersensitivity ratio was shown to decrease with increasing alkaline earth size, hence decreasing cation field strength, in the 40 AEO – 60 SiO_2 (AE = Ca, Sr, Ba) system [19]; similar to the dependence found here in the nanoparticles prior to doping and processing in the silica glass.

#174771 - $15.00 USD Received 23 Aug 2012; revised 24 Sep 2012; accepted 26 Sep 2012; published 1 Oct 2012

This difference in surroundings is consistent with the as-made nanoparticles and suggests that the SrF_2 and BaF_2 nanoparticles are more influenced by the surrounding SiO_2 matrix, due to the larger volume they occupy upon incorporation and subsequently diffuse into at elevated temperatures. The change in emission behavior between the conventional solution doped preform and the nanoparticle doped preforms suggest that the nanoparticles, though inevitably oxidized during the high temperature MCVD process, yield a spatial localization of the rare earth ion in the glass host, and the rare earth ion largely remains near the volume originally comprised by the nanoparticle.

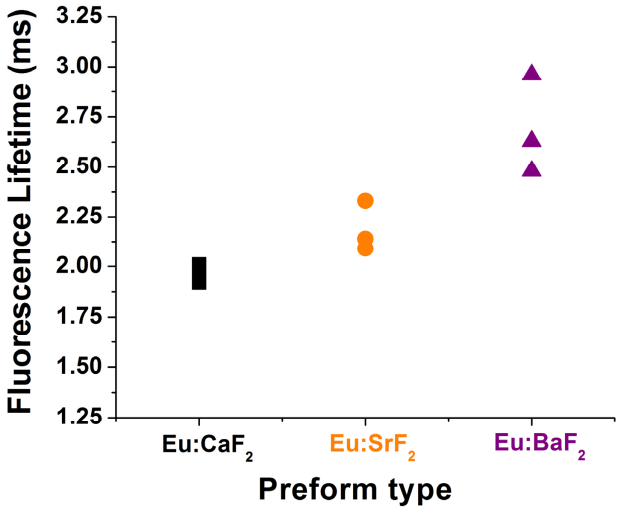

Fig. 4. Comparison of the lifetime values for each type of Eu:AEF_2-doped preform. Since the conventionally-prepared preform exhibited only Eu^{2+} emissions, similar data could not be obtained as it is relates to the Eu^{3+} dynamics.

The influence of the change in environment is further evidenced by the analysis of the vibrational energies of the different alkaline earth systems studied. Spontaneous Raman scattering analysis (not shown) of the as-made and heat-treated nanoparticles yielded vibrational energies of 320 cm^{-1} (CaF_2), 282 cm^{-1} (SrF_2), and 240 cm^{-1} (BaF_2), respectively, for the as-made fluoride nanoparticles and 965 cm^{-1} (CaF_2-derived), 950 cm^{-1} (SrF_2-derived), and 936 cm^{-1} (BaF_2-derived), respectively, for the heat-treated samples. These latter values are similar to those reported previously for alkaline-earth oxides [20]. The observed trend of reduced vibrational energy with increasing cationic mass is expected. Further, these results clearly suggest, as would be expected, that there is oxidation of the alkaline earth fluoride nanoparticle during the subsequent thermal processing. That said, it is interesting to note that certain vibrations associated with the alkaline earth fluorides still are present in the heat treated nanoparticles, indicating that complete oxidation of the fluoride nanoparticles does not take place. Further, in comparing the different alkaline earth hosts, the environments can be viewed as completely different, supporting the postulation that the incorporation of rare earths via alkaline earth fluoride nanoparticle hosts provides a predictable localized environment for the rare earth ion, and in turn, a method to predetermine and tailor the emissions of an optical glass fiber.

Radiative lifetime measurements on the Eu:AEF_2-doped preforms were performed in order to determine whether or not the local chemistry associated with the nanoparticle doping influenced the spectroscopic properties of the dopant. The resultant first e-folding times for three measurements on the Eu:$(AE)F_2$ doped preforms are shown in Fig. 4. The higher vibrational energy of the CaF_2 as compared to SrF_2 and BaF_2 is an indication of the shorter lifetime exhibited and the difference in the surroundings from one host material to the next. In

#174771 - $15.00 USD Received 23 Aug 2012; revised 24 Sep 2012; accepted 26 Sep 2012; published 1 Oct 2012

glasses with low vibrational energy, the europium ions typically reside in a more ionic local environment which supports relatively long fluorescent lifetime.

The fact that the lifetime values can be tuned by nanoparticle composition is quite extraordinary. Specifically, there is a measurable lengthening of the radiative lifetime with increasing mass of the nanoparticle constituent cation, further supporting the premise that the environment about the dopant ion is dominated by the original nanoparticle matrix, with less influence from the silica glass matrix. In this case treated here, the average (slower decay) radiative lifetime for the CaF_2, SrF_2, and BaF_2 solution doped preforms is 1.96 ms, 2.19 ms, and 2.69 ms, respectively; a difference of about 37%. Of greatest practical consequence is that one clearly can control the radiative lifetime of dopants in otherwise "conventional" silica preforms.

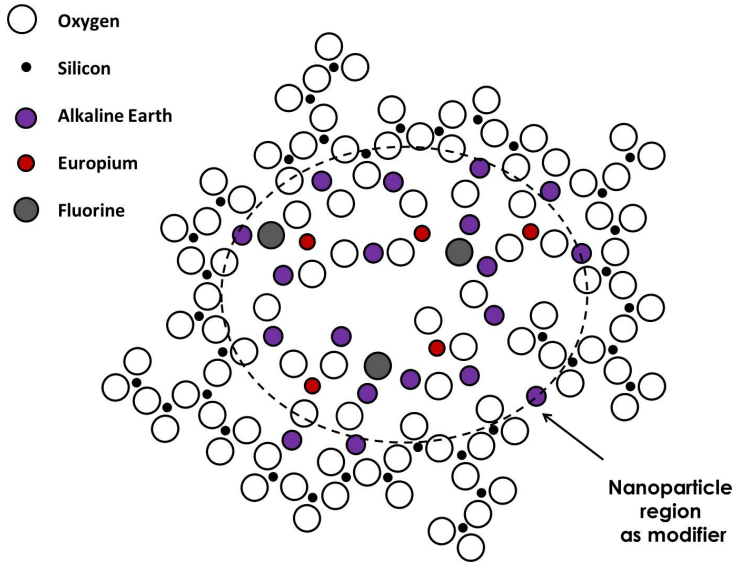

Fig. 5. Two-dimensional schematic representation of the incorporation of Eu:(AE)F_2 nanoparticles into the silica optical fiber preform based on the vibrational, phonon sideband, and fluorescence data.

Based on the results noted above, Fig. 5 provides a generalized (two dimensional) schematic representation of the possible local structural environment of the rare earth within the core region of the silica optical fiber preform. This generalization is quite different from that proposed previously for nanoparticle-doped glasses [14]. It is evident that the general chemistry of the nanoparticle persists, including some of the fluorine, and that the cations play an important role in the vibrational environment around the rare-earth dopant. It also is known that there is diffusion of the nanoparticle species during the thermal processing [18] such that some of the silicon and oxygen would be present in the immediate vicinity of the rare earth dopant.

While more detailed work needs to be done to quantify the exact local environment about the active dopant, it is clear that differing nanoparticles influence the spectroscopic properties of the resultant silica preform differently. Further, since the active dopants will not diffuse to the point where they are uniformly dispersed through-out the silica preform; i.e., they remain in reasonable proximity to the original nanoparticle, including its (potentially heavy) cations, so that one can achieve the benefits of locally-high doping yet globally low effective concentration. An example where this might be useful could be thulium-based eye-safe fiber lasers where one needs high Tm^{3+} doping to permit the cross-relaxations that facilitate efficient emissions at 2 μm. Through nanoparticle doping, one conceivably could use a highly Tm-doped nanoparticle such that there is efficient cross-relaxation at the ion-ion level but a low overall Tm concentration to lower loss and thermal load. Additionally, as is known from

#174771 - $15.00 USD Received 23 Aug 2012; revised 24 Sep 2012; accepted 26 Sep 2012; published 1 Oct 2012

[15], nanoparticles doped with different active ions also can be introduced into the same preform to permit (or preclude) energy transfer between dopants. So this ability to control energy transfer between differing dopants and, now, influence spectroscopy through nanoparticle chemistry, provides useful and effective additional methods to enhance the performance of active optical fibers.

4. Conclusions

Europium-doped alkaline earth fluoride nanoparticles were successfully used as solution doping delivery materials for the fabrication of silica optical fiber preforms. The spectral emissions of the nanoparticle doped preforms were characteristic of trivalent europium, Eu^{3+}, which is counter to conventional dissolved salt methods where only Eu^{2+} is formed without considerable compositional modification. Distinct differences were observed in the vibrational and spectroscopic behaviors depending on the alkaline earth ion used indicating that the local chemical and structural environment about the dopant ion can be influenced by the nature of the nanoparticle employed. Fluorescence lifetimes of the nanoparticle doped preforms were shown to increase with decreasing vibrational energy of the nanoparticle host material, indicating the local chemical environment of the dopant nanoparticle is retained somewhat in the resultant optical fiber preform. A more reasonable local structural model of the doped core glass region has been developed based on the measured properties and suggests that the rare earth ion is relatively 'insulated' from the surrounding silica matrix by the immediate surroundings associated with the original nanoparticle host. Overall, it has been shown that the use of rare earth doped nanoparticles can provide additional and useful performance factors relative to conventional dissolved salt solution doping methods for active optical fiber.

#174771 - $15.00 USD Received 23 Aug 2012; revised 24 Sep 2012; accepted 26 Sep 2012; published 1 Oct 2012